Atmospheric Oxidation Pathways of Acetic Acid

Claudette M. Rosado-Reyes and Joseph S. Francisco*

Department of Chemistry and Department of Earth and Atmospheric Sciences, Purdue University, West Lafayette, Indiana 47907

Received: November 23, 2005; In Final Form: February 7, 2006

One of the most abundant carboxylic acids measured in the atmosphere is acetic acid ($CH_3C(O)OH$), present in rural, urban, and remote marine environments in the low-ppb range. Acetic acid concentrations are not well reproduced in global 3-D atmospheric models because of the poor inventory of sources and sinks to model its global distribution. To understand the complete oxidation of acetic acid in the atmosphere initiated by OH radicals, ab initio calculations are performed to describe in detail the energetics of the reaction potential energy surface (PES). The proposed reaction mechanism suggests that the $CH_3C(O)OH + OH$ reaction takes place via three pathways: the addition of OH to the central carbon, the abstraction of a methyl hydrogen, and the abstraction of an acidic hydrogen. The PES is characterized by prereactive H-complexes, transition states, and more interestingly unique radical-mediated isomerization reactions. From the analysis of the energetics, acetic acid atmospheric oxidation will proceed mainly via the abstraction of the acidic hydrogen, consistent with previous experimental and theoretical studies. The major byproducts from each pathway are identified. Glyoxylic acid is suggested to be a major byproduct of the atmospheric oxidation of acetic acid. The atmospheric fate of glyoxylic acid is discussed.

Introduction

Carboxylic acids are ubiquitous and important chemical components of the troposphere.[1] Carboxylic acids contribute significantly to the acidity of atmosphere precipitation, up to 64%, and a large fraction (∼25%) to the nonmethane hydrocarbon atmospheric mixture.[2] They have been found in gaseous and aqueous phases, and in aerosol particles. Dry and wet deposition serves as their major sink in the atmosphere. They are also involved in important atmospheric heterogeneous transformations. The relative importance of natural and anthropogenic sources of carboxylic acids is still not well established at a regional and global scale, and is the subject of recent laboratory and field studies.[1]

One of the most abundant carboxylic acids measured in the atmosphere is acetic acid. Concentrations of acetic acid have been reported in the ppb range in urban, semirural, and rural areas,[3−9] and in remote marine regions.[10,11] In atmospheric aerosols, concentrations of acetate ion have been measured in the low (0.5−40) ppt range.[12,13] It has been shown that more than 91% of the total acetic acid concentration is present in the gas phase,[14,15] assuming that volatile organic acids would incorporate into the aerosol surface by adsorption.[16] Dry deposition has been identified as a major loss process for organic acids (formate and acetate) in the gas phase,[2] accounting for 91% of the total acetic acid deposition budget in Southern California,[3] and 51% in the tropical Venezuelan savannah region.[6]

Acetic acid is released from different sources. Biomass burning represents a direct source from anthropogenic emissions. Talbot et al.[4] showed the biomass combustion represents a source of carboxylic acids, especially acetic acid, in the atmosphere. During a biomass burning event (fresh vegetation, dried wood) at a natural site, concentrations ranging from 3000 to 5000 ppbv were measured for acetic acid. These concentrations were 2 to 3 orders of magnitude higher than ambient concentration in the same area away from the burning site, concluding that biomass burning is an important direct source of acetic acid in the atmosphere.

Acetic acid has been measured in automobile exhaust. Kamura et al.[17] determined the presence and distribution of organic acids (C1−C10) in the atmosphere, motor exhaust, and engine oils. The results showed that acetic acid was the most abundant species followed by formic and propionic acids in the atmosphere. Motor exhaust was shown as a major source of organic acids, where also acetic acid was the most abundant, followed by formic and propionic acids. Concentrations were 17 times higher in the motor exhaust than in the atmosphere. These organic acids were also identified in engine oils. In new engine oils the content of carboxylic acids was negligible prior to their use. On the other hand, the content in used oils was major, suggesting that they are produced by incomplete combustion of gasoline and then scavenged from the combustion chamber into lubricating oil.

Biogenic sources are also considered, which include the direct emission from soil[18,6] and vegetation[16,19−24] and possibly bacteria metabolism in cloud droplets.[25] From the vertical distribution investigation of formic and acetic acids concentration in Germany's forested areas, the results of Enders et al.[18] suggested that soil emissions may be a major source of monocarboxylic acids in the atmosphere. Talbot et al.[12] concluded that emissions from vegetation in the Amazonian forest in Brazil contribute up to 50% of the tropospheric concentrations of main carboxylic acids (formic and acetic acids).

Reaction of ozone with alkenes has been studied as a source of carboxylic acids. Some of these alkenes are naturally occurring olefins. Olefins are emitted primarily by soil and vegetation. Among different olefins, isoprene and monoterpenes (α- and β-pinenes) are the most abundant. Olefins are also emitted from the ocean surface in marine atmospheres. Also, in terms of the production of nonmethane hydrocarbons from

10.1021/jp0567974 CCC: $33.50
Published on Web 03/11/2006

marine sources, light alkenes predominated in the distribution. Ozone reacts with alkenes in the gas phase to produce an unstable ozonide

$$O_3 + RCH{=}CH_2 \rightarrow \quad (1)$$

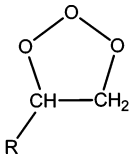

The unstable ozonide decomposes in two different ways to produce a carbonyl compound and a reactive Criegee intermediate (biradial)

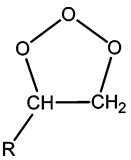

$$\rightarrow RC(O)H + {}^{\bullet}CH_2COO^{\bullet} \quad (2)$$

$$\rightarrow HC(O)H + {}^{\bullet}RHCOO^{\bullet} \quad (3)$$

The Criegee intermediate contains excess energy. It can either decompose unimolecularly to produce small products and free radicals or stabilize by collisions and isomerize to produce the corresponding carboxylic acid

$$({}^{\bullet}RHCOO^{\bullet})^* \rightarrow \text{fragments} \quad (4)$$

$$\xrightarrow{M} RC(O)OH \quad (5)$$

In the lower troposphere where water vapor concentrations are high, the Criegee intermediate can react in the following manner

$${}^{\bullet}RHCOO^{\bullet} + H_2O \rightarrow RC(O)OH + H_2O \quad (6)$$

$$\xrightarrow{M} RCH(O)OOH \quad (7)$$

$$\rightarrow RC(O)OH + H_2O \quad (8)$$

$$\rightarrow RC(O)H + H_2O_2 \quad (9)$$

Water vapor catalyzes the rearrangement of the Criegee intermediate to produce carbonyl compounds and carboxylic acids. In the above mechanism, if R is a methyl group, acetic acid is obtained as product.

Acetic acid can also be produced from acetylperoxy radical reactions. Acetylperoxy radicals are formed in the atmosphere during the photooxidation of carbonyl compounds such as acetone, acetaldehyde, methyl vinyl ketone, methylglyoxal, etc.[26] In urban environments, they react with NO_2 to produce peroxyacetyl nitrate (PAN), an important constituent of photochemical smog. At low temperatures, PAN is thermally stable. At such conditions PAN acts as a reservoir for NO_x and so it is responsible for transporting nitrogen oxides through the troposphere. In rural environments, acetylperoxy radicals react with other peroxy radicals.

Previous experimental and modeling studies have proposed the reactions of acetylperoxy radicals with hydroperoxy radicals HO_2,[27,28] methyl peroxy radicals CH_3OO,[26] and other primary or secondary peroxy radicals RR′CHOO,[29] as a source of acetic acid

$$CH_3C(O)O_2 + HO_2 \rightarrow CH_3C(O)OH + O_3 \quad (10a)$$

$$\rightarrow CH_3C(O)OOH + O_2 \quad (10b)$$

$$CH_3C(O)O_2 + CH_3O_2 \rightarrow CH_3C(O)OH + O_2 + HC(O)H \quad (11a)$$

$$\rightarrow CH_3 + CO_2 + O_2 + CH_3O \quad (11b)$$

$$CH_3C(O)O_2 + RR'CHO_2 \rightarrow CH_3C(O)OH + O_2 + RC(O)R' \quad (12a)$$

$$\rightarrow CH_3 + CO_2 + O_2 + RR'CHO \quad (12b)$$

Since peroxy radicals have been measured in large quantities in the atmosphere, reactions 10−12 are expected to be potential and significant sources of acetic acid. Niki et al.[27] determined with FTIR spectroscopy that reaction 10a accounted for 25% of the total product yield from reaction 10. The production of acetic acid was observed in the solution phase. The kinetics of reaction 10 has been examined by Moortgat et al.[28] at atmospheric pressure and 253−368 K by flash photolysis UV spectroscopy. An overall rate constant expression of $k_{10} = (4.3 \pm 1.2) \times 10^{-13} \exp[(1040 \pm 100)]/T$ cm^3 molecule^{-1} s^{-1} and a branching ratio k_{11a}/k_{11} equal to 0.33 ± 0.07 were calculated from kinetic simulations. Moortgat and co-workers[26] studied the kinetics of reaction 11 by flash photolysis UV absorption spectroscopy and an equal contribution of both branches to the overall rate constant was deduced at room temperature by kinetics model simulations: $k_{11a} = k_{11b} = 5.5 \times 10^{-12}$ cm^3 molecule^{-1} s^{-1}. Reaction 11a was first proposed by Kenley and Traylor.[30] The contribution of reactions 10−12 to the production of acetic acid in the Amazon boundary layer was evaluated by a coupled photochemical-dynamical 1-D model to simulate field experiment concentrations of acetic acid raging between 1 and 5 ppbv.[31] The modeling results, although subjected to a large uncertainty, indicated that acetyl radical chemistry can produce acetic acid concentrations of several ppbv, comparable to the experimentally observed values.

The production of acetic acid has also been postulated from the reaction of acetone with OH radicals. The previous investigation by Wollenhaupt et al.[32,33] of the acetone + OH rate constant showed a non-Arrhenious behavior below 240 K. The negative temperature dependence was explained by proposing that the reaction proceeds via two parallel paths: hydrogen abstraction, favored at higher temperatures, or addition of OH followed by CH_3 elimination, favored at lower temperatures.[32]

$$CH_3C(O)CH_3 + OH \rightarrow CH_3C(O)CH_2 + H_2O \quad (13a)$$

$$\rightarrow (CH_3)_2C(OH)O^{\bullet} \rightarrow CH_3 + CH_3C(O)OH \quad (13b)$$

Subsequently, a branching ratio k_{13b}/k_{13} of 0.5 ± 0.15 at 298 K and 0.3 ± 0.1 at 233 K was determined by means of quantifying CH_3O concentrations by pulsed laser induced fluorescence.[33] In contrast with Wollenhaupt and co-workers'[32,33] previous observations, these results showed a positive temperature dependence on the branching ratio of OH-addition vs H-abstraction. Vasvári et al.[34] reported a branching fraction k_{13a}/k_{13} of 0.5 ± 0.04 at room temperature by probing $CH_3C(O)CH_2$ radicals with laser induced fluorescence. However, Vandenberk et al.[35] determined $k_{13b}/k_{13} \sim 5\%$ with no significant measurable acetic acid concentrations via flow-reactor beam sampling mass spectrometry. By using density functional theory calculations and transition state theory and RRKM analyses, it was determined that the OH-addition channel leading to the production of acetic acid is insignificant under atmospheric

conditions. It is still not clear to what extent acetone atmospheric degradation contributes to the production of acetic acid.

Several attempts in understanding the mechanism for the reaction of carboxylic acids with OH radicals have proposed that the reaction proceeds via a complex rather than a direct mechanism.[36−38] Experimental studies of the kinetics and mechanism of the reaction of hydroxyl radicals with formic and deuterated formic acids showed that the estimated $k_{HC(O)OH+OH}$ was independent of total pressure (30−500 Torr) and O_2 concentrations, temperature independent between 298 and 430 K, and sensitive to deuterium substitution for the acidic hydrogen, but independent of deuterium substitution at the formyl carbon. Also an overall activation barrier of zero or slightly negative was observed for the reaction. These observations led to the conclusion that OH reacts initially through addition and then abstraction and that it must interact preferentially with the acidic hydrogen. This preferential interaction was confirmed by the very low reactivity of formic and deuterated formic acid dimers toward the OH radical relative to the monomer. On the basis of these results, a two-channel reaction mechanism was proposed for the reaction of formic acid with OH radicals. The proposed mechanism involves (1) formation of a hydrogen-bonded complex between OH and formic acid followed by the abstraction of the carboxylic hydrogen, (2) direct abstraction of the formyl hydrogen

$$HC(O)OH + OH \leftrightarrow [HC(O)O-H-OH] \rightarrow HC(O)O + H_2O \quad (14)$$

$$HC(O)O \rightarrow H + CO_2 \quad (15)$$

$$HC(O)OH + OH \rightarrow C(O)OH + H_2O \quad (16)$$

$$C(O)OH \rightarrow H + CO_2 \quad (17)$$

Galano et al.[39] investigated the rate coefficient and mechanism of the gas-phase OH hydrogen abstraction reaction from formic acid by ab initio methods. The reaction mechanism was analyzed in terms of the stability of reactants, prereactive complexes, and transition state structures participating in the chemical reaction. In agreement with experimental results, the existence of the two channels explained the non-Arrhenius behavior of the reaction. A large calculated tunneling factor supported the conclusion that the acidic channel was more stable with a narrower but higher transition state energy barrier and the largest contribution to the overall rate constant.

In global three-dimensional atmospheric models acetic acid concentrations are not well reproduced.[40] The model underestimated acetic acid concentrations by a factor of ∼3−9 compared to concentrations of 200−500 pmol/mol measured over the Atlantic. A photochemical source of 75 Tg/yr was calculated, considerably smaller than the 120 Tg/yr previously reported. These major discrepancies supported the fact that the global cycle (sources and sinks) of acetic acid is not well understood. An accurate enough inventory of sources and sinks for organic acids is not currently available to model the global distribution of these compounds.[41]

The kinetics and degradation of acetic acid has been previously studied.[42−44] Dagaut et al.[42] measured the rate constant for the gas-phase reactions of OH radicals with a series of carboxylic acids in a flash photolysis resonance fluorescence apparatus over the temperature range 240−440 K. An Arrhenius dependence was derived for the $CH_3C(O)OH + OH$ reaction of $k = (1.3 \pm 0.1) \times 10^{-12} \exp[-(170 \pm 20)/T]$ cm^3 molecule^{-1} s^{-1}. Singleton et al.[43] estimated rate constants for the reactions of hydroxyl radicals with the monomer and dimer of acetic acid, deuterated acetic acid, and propionic acid by laser photolysis-resonance absorption spectroscopy at temperatures of 297−445 K. The estimated room temperature value of $k_{CH_3C(O)OH+OH} \sim 2.03 \times 10^{-11}$ cm^3 molecule^{-1} s^{-1} was higher by 14% than the value previously reported by Dagaut and co-workers.[42] On the basis of the analysis of the bond dissociation energies of O−H and C−H of the acids and the equilibrium constant for the formation of the OH−carboxylic acid complex, the results were consistent with the two-channel reaction mechanism initially proposed for the reaction of formic acid with OH radicals. The need for further evaluation of the reaction mechanism by theoretical calculations of structures and potential energies of the intermediates of all possible channels was addressed. Butkovskaya et al.[44] determined the overall rate constant of the $CH_3C(O)OH + OH$ reaction in the temperature range of 229−300K using chemical ionization mass spectrometry coupled to a high turbulent flow reactor. The following reaction mechanism was investigated

$$OH + CH_3C(O)OH \rightarrow CH_3 + CO_2 + H_2O \quad (18a)$$

$$\rightarrow CH_2C(O)OH + H_2O \quad (18b)$$

The rate constant showed a strong negative temperature dependence, consistent with the formation of the $OH{\cdot}CH_3C(O)OH$ prereactive complex proposed previously for the reaction of formic acid with OH. An Arrhenius expression of $k_{18}(T) = [(2.2 \pm 0.2) \times 10^{-14} \exp(1012 \pm 80)/T]$ was derived. On the basis of CO_2 yields, a branching ratio of $k_{18a}/k_{18} = (64 \pm 17)\%$ was determined at temperatures between 249 and 300 K.

To date, there is only one study where the product distribution of the reaction of acetic acid with hydroxyl radicals was investigated theoretically, and the branching ratio for the abstraction of the acidic hydrogen was determined experimentally based on measured CO_2 yields by the mass spectrometry technique.[45] The potential energy surface was explored in detail up to the formation of the alkyl radical from the hydrogen abstraction and OH-addition channels. A large uncertainty was obtained in the H-abstraction characteristics of the transition states, especially for the abstraction of the acidic hydrogen. Second-order Møller−Plesset perturbation (MP2) theory and the Becke three-parameter hybrid functional combined with Lee, Yang, and Parr correlation (B3LYP) density functional theory methods did not provide enough accuracy on structures and vibrational frequency analysis to fully reproduce the previous experimental findings of temperature-dependent rate constants and branching ratios.

It is then of relevance to understand acetic acid and byproducts oxidation mechanisms in the atmosphere, initiated by OH radicals. This present study intends to evaluate the $CH_3C(O)OH + OH$ reaction mechanism by ab initio molecular orbital calculation and to identify the main products of the atmospheric oxidation of acetic acid.

Computational Methods

Gaussian 98 and 03 suites of programs[46] were utilized to perform ab initio molecular orbital calculations on acetic acid, radical, prereactive complex, and transition state structures. Geometry optimizations and frequency calculations were carried out by using the levels of theory of second-order Møller−Plesset perturbation (MP2,full) and quadratic configuration interaction with singlets and doubles (QCISD) with the 6-31G(d) basis set to find equilibrium geometries, vibrational frequencies, and zero point energies. All optimizations were carried out to better than

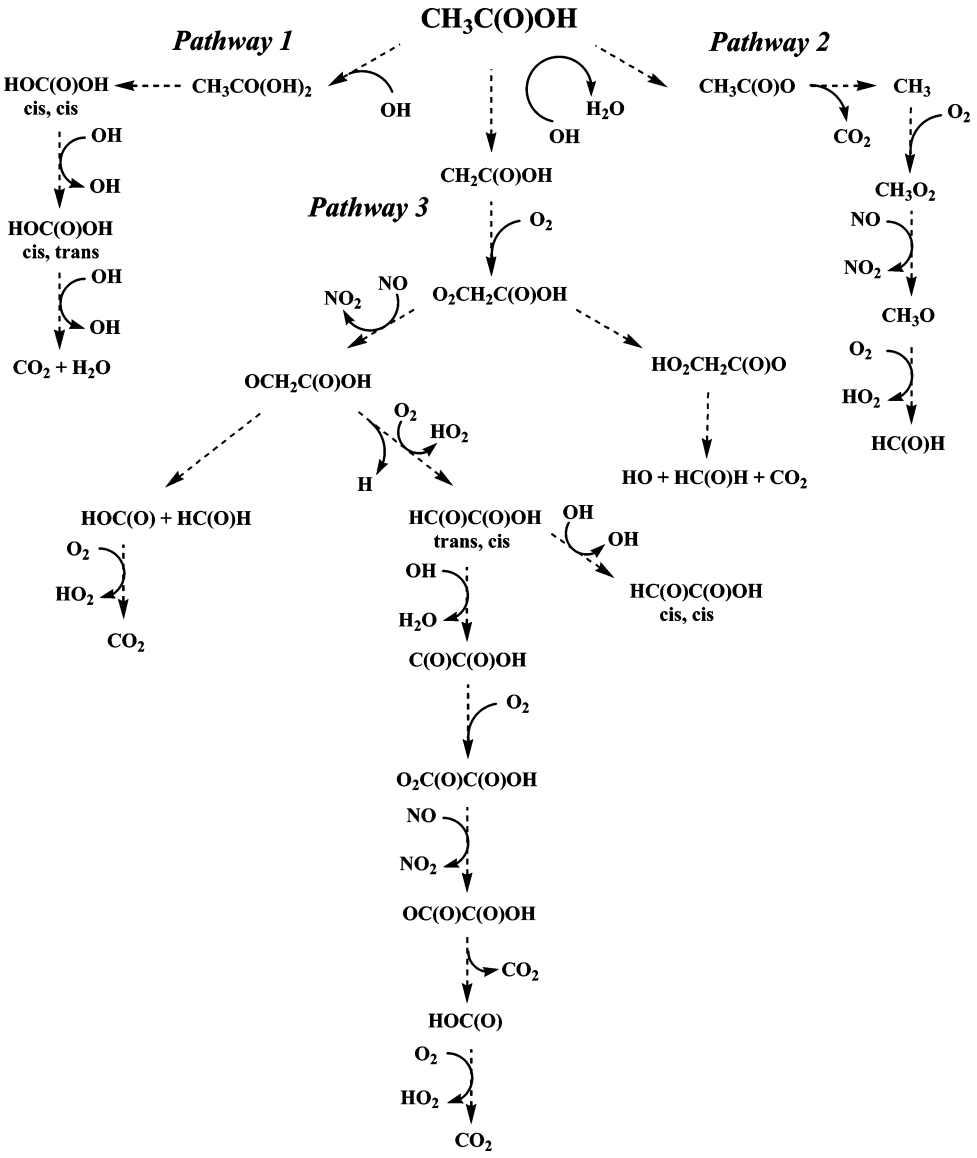

Figure 1. Atmospheric degradation pathways for acetic acid.

0.001 Å for bond lengths and 0.1° for angles, with a self-consistent-field convergence criteria of at least 10^{-7} on the density matrix and a residual rms (root-mean-square) force of less than 10^{-4} au. Harmonic vibrational frequencies, obtained with analytical second derivatives for the optimized minimum energy geometries, confirmed true minima and first-order saddle points. Global minima had all positive frequencies while one imaginary frequency was found for each transition state, confirming their location as maxima in one reaction coordinate. The proper connectivity between reactants, prereactive complexes, transition states, and products were verified by intrinsic reaction coordinate calculations (IRC). To refine energy values of equilibrium geometries, two single-point calculations with higher levels of electron correlation, i.e., quadratic configuration including singles, doubles, and perturbative corrections for triplets [QCISD(T)], were performed with the 6-31++G(2d,-2p) and 6-31++G(2df,2p) basis sets. The degree of spin contamination was monitored because of the possible production of inaccurate total energies. For open shell systems the $\langle S^2 \rangle$ value did not have major deviations from 0.75.

Enthalpies of reaction ($\Delta H_{r,0}$) and barrier heights, corrected with zero-point energies (ZPE), were calculated to characterized the energetics of the potential energy surface of the reaction of $CH_3C(O)OH$ with OH radical.

Results and Discussion

The proposed reaction mechanism for the $CH_3C(O)OH$ + OH reaction is depicted in Figure 1. The reaction under examination consists of three different pathways. Pathway 1 describes the addition of an OH radical to the central carbonyl carbon atom. Pathway 2 consists of the abstraction of the acidic hydrogen, at the carboxylic acid side, by OH radicals. Pathway 3 involves the hydrogen abstraction by OH radicals from the methyl group. The results will be discussed and analyzed in terms of the mechanistic pathways. Absolute energies of optimized geometries are shown in Table S1 (Supporting Information). Vibrational frequencies and zero-point energy corrections of species, prereactive complexes, and transition states are included in Table S2 (Supporting Information). Enthalpies of reaction and activation barriers are listed in Table 1. Table 2 shows the binding energies of prereactive complexes.

A. Mechanistic Analysis of the Atmospheric Oxidation of Acetic Acid. *Pathway 1.* The structures of closed- and open-shell species, prereactive complexes, and transition states are

TABLE 1: Enthalphies of Reactions and Activation Barriers According to the Proposed Mechanism[a]

					QCISD(T)/					
	MP2(full) 6-31G(d)		QCISD/ 6-31G(d)		6-31++G(2d,2p)		6-31++G(2df,2p)		G2M(CC,MP2)//B3LYP/ 6-311++G(2df,2pd)[b]	
chemical reactions	$\Delta H_{r,0}$	barrier height	$\Delta H_{r,0}$	barrier height	$\Delta H_{r,0}$	barrier height	$\Delta H_{r,0}$	barrier height	$\Delta H_{r,0}$	barrier height
pathway 1										
$CH_3C(O)OH + OH \rightarrow CH_3CO(OH)_2$	0.2	15.5	0.4	13.3	−0.5	8.2	−0.5	9.5	−0.8	9.5
$CH_3CO(OH)_2 \rightarrow HOC(O)OH + CH_3$	−20.7	10.0	−14.5	10.6	−16.6	6.2	−16.1	6.1	−15.4	6.1
$HOC(O)OH_{cis,cis} + OH \rightarrow HOC(O)OH_{cis,trans} + OH$	1.9	3.6	1.9	9.3	1.6	4.4	1.6	6.7		
$HOC(O)OH + OH \rightarrow CO_2 + OH + H_2O$	−9.4	16.1	−6.6	23.9	−12.1	40.3	−10.1	42.7		
pathway 2										
$CH_3C(O)OH + OH \rightarrow CH_3C(O)O + H_2O$	−1.9	6.7	−5.8	7.4	−3.8	−0.0	−2.4	2.1	−6.7	1.6
$CH_3C(O)O \rightarrow CO_2 + CH_3$	−26.1	7.3	−13.0	9.2	−23.7	−3.1	−22.7	−2.7	−16.2	−2.3
$CH_3 + O_2 \rightarrow CH_3O_2$	−18.8		−26.8		−25.9		−28.5			
$CH_3O + NO \rightarrow CH_3O + NO_2$	−21.4		−0.2		−12.4		−13.9			
$CH_3O + O_2 \rightarrow HC(O)H + HO_2$	−18.7	40.0	25.6	19.9	−25.6	17.5	−26.0	17.0		
pathway 3										
$CH_3C(O)OH + OH \rightarrow CH_2C(O)OH + H_2O$	−14.1	8.1	−10.8	11.1	−20.2	2.4	−18.5	4.0	−18.5	4.0
$CH_2C(O)OH + O_2 \rightarrow O_2CH_2C(O)OH$	−14.2	−	−19.2		−18.9		−21.3			
$O_2CH_2C(O)OH + NO \rightarrow OCH_2C(O)OH + NO_2$	−23.3	−	−6.5		−7.4		−8.9			
$OCH_2C(O)OH + O_2 \rightarrow HC(O)C(O)OH + HO_2$	−20.2	48.7	−21.8	28.8	−33.1	6.5	−33.4	6.1		
$OCH_2C(O)OH \rightarrow HC(O)C(O)OH + H$	4.1	26.2	15.2	24.8	12.1	17.4	11.9	17.0		
$OCH_2C(O)OH \rightarrow HOC(O) + HC(O)H$	6.7	24.5	10.8	20.2	2.6	9.4	3.8	10.0		
$HOC(O) + O_2 \rightarrow CO_2 + HO_2$	−42.0	10.3	−45.7	10.1	−47.5	4.2	−48.6	2.8		
$O_2CH_2C(O)OH \rightarrow HO_2CH_2C(O)O$	25.5	36.3	22.1	26.9	25.8	27.6	26.0	26.4		
$HO_2CH_2C(O)O \rightarrow CO_2 + HC(O)H + OH$	−66.4		−57.9		−64.2		−63.7			
$HC(O)C(O)OH + OH \rightarrow C(O)C(O)OH + H_2O$	−25.4	10.4	−19.1	5.4	−29.5	−4.1	−27.7	−2.0		
$C(O)C(O)H + O_2 \rightarrow O_2C(O)C(O)OH$	−8.0		−12.4	−	−24.7		−27.0			
$O_2C(O)C(O)OH + NO \rightarrow OC(O)C(O)OH + NO_2$	−39.5		−28.3		−19.8		−21.7			
$OC(O)C(O)OH \rightarrow HOC(O) + CO_2$	−34.5	2.2	−23.1	2.5	−27.8	−0.1	−27.8	0.0		
HC(O)C(O)OH trans,cis + OH → HC(O)C(O)OH cis,cis + OH	0.8	4.4	0.8	10.4	1.1	20.1	1.1	22.2		

[a] Values in kcal/mol. [b] De Smedt et al.[45]

TABLE 2: Binding Energies (in kcal/mol) of Complexes

prereactive complex	reaction pathway	this work[a]	ref 45[b]
CX1	P2: $CH_3C(O)OH + OH \rightarrow CH_3C(O)O + H_2O$	6.5	7.3
CX2	P3: $CH_3C(O)OH + OH \rightarrow CH_2C(O)OH + H_2O$	4.4	5.1
CX3	P3: $HC(O)C(O)OH_{trans,cis} + OH \rightarrow C(O)C(O)OH + H_2O$	3.2	
CX4	P3: $HC(O)C(O)OH_{trans,cis} + OH \rightarrow HC(O)C(O)OH_{cis,cis} + OH$	2.1	

[a] QCISD(T)/6-31++G(2df,2p)//QCISD/6-31G(d). [b] G2M(CC,MP2)//B3LYP/6-311++G(2df,2pd).

illustrated in Figure 2. Acetic acid (Figure 2a) geometry is characterized by two hydrogen atoms, one acidic and one methyl, aligned in a plane ($\tau = 0$) with the carbonyl oxygen atom. The transition state structure of the addition of OH radicals to the central carbonyl carbon atom of acetic acid is shown in Figure 2r. The C═O bond elongates by 0.06 Å while the CO oxygen atom leans back to accommodate the incoming OH radical, keeping dihedral angles of 21° and 36° with the acidic and methyl hydrogens, respectively. In the product resulting from this initial step, $CH_3CO(OH)_2$ (Figure 2b), the carbonyl CO bond stretches to 1.389Å, and a methyl hydrogen is oriented trans with respect of the center CO oxygen atom. Both carboxylic CO bonds, with bond lengths of 1.390 and 1.414 Å, are oriented in the same fashion with respect to the central CO bond with dihedral angles of 77° and 39°, respectively. It is expected that the $CH_3CO(OH)_2$ radical will eject a methyl radical to produce carbonic acid [HOC(O)OH]. Carbonic acid is produced in its most stable configuration, cis-cis (Figure 2c). The symmetric geometry is characterized by equivalent COH groups, coplanar to the central carbonyl group, and CO and OH bond lengths of 1.343 and 0.975 Å, respectively. The structure of carbonic acid has been previously studied during extensive theoretical investigations of its formation from water and carbon dioxide,[47,48]

$$H_2O + CO_2 \rightarrow HOC(O)OH \qquad (19)$$

The carbonic acid geometry parameters calculated at the MP2-(full)/6-31++G(d,p) level are in very good agreement with ours, which are calculated at QCISD/6-31G(d).

Interestingly, during this study it was found that OH radicals can participate as mediators during the radical induced isomerization reaction. An OH radical molecule can assist in the exchange of a proton on carboxylic acids. Figure 2t shows the transition state for this reaction, an alternative route for isomerization from the HOC(O)OH most stable configuration (global minimum) to its local minimum via an intermolecular OH-assisted proton transfer from one oxygen to the other. In the transition state structure both CO bonds gain some partial double bond character and the transference of two hydrogen

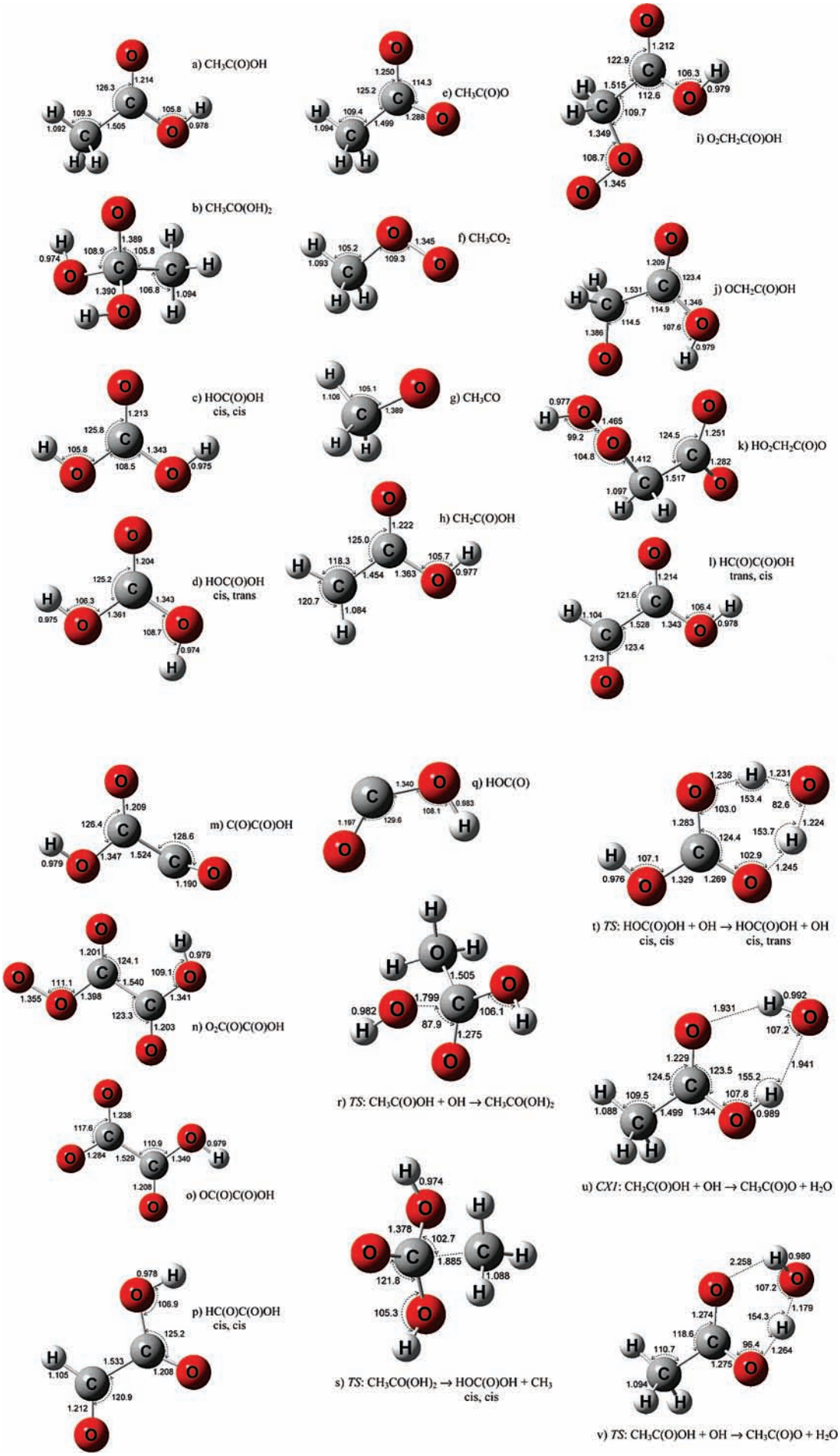
a) CH3C(O)OH
b) CH3CO(OH)2
c) HOC(O)OH cis, cis
d) HOC(O)OH cis, trans
e) CH3C(O)O
f) CH3CO2
g) CH3CO
h) CH2C(O)OH
i) O2CH2C(O)OH
j) OCH2C(O)OH
k) HO2CH2C(O)O
l) HC(O)C(O)OH trans, cis
m) C(O)C(O)OH
n) O2C(O)C(O)OH
o) OC(O)C(O)OH
p) HC(O)C(O)OH cis, cis
q) HOC(O)
r) TS: CH3C(O)OH + OH → CH3CO(OH)2
s) TS: CH3CO(OH)2 → HOC(O)OH + CH3 cis, cis
t) TS: HOC(O)OH + OH → HOC(O)OH + OH cis, cis cis, trans
u) CX1: CH3C(O)OH + OH → CH3C(O)O + H2O
v) TS: CH3C(O)OH + OH → CH3C(O)O + H2O

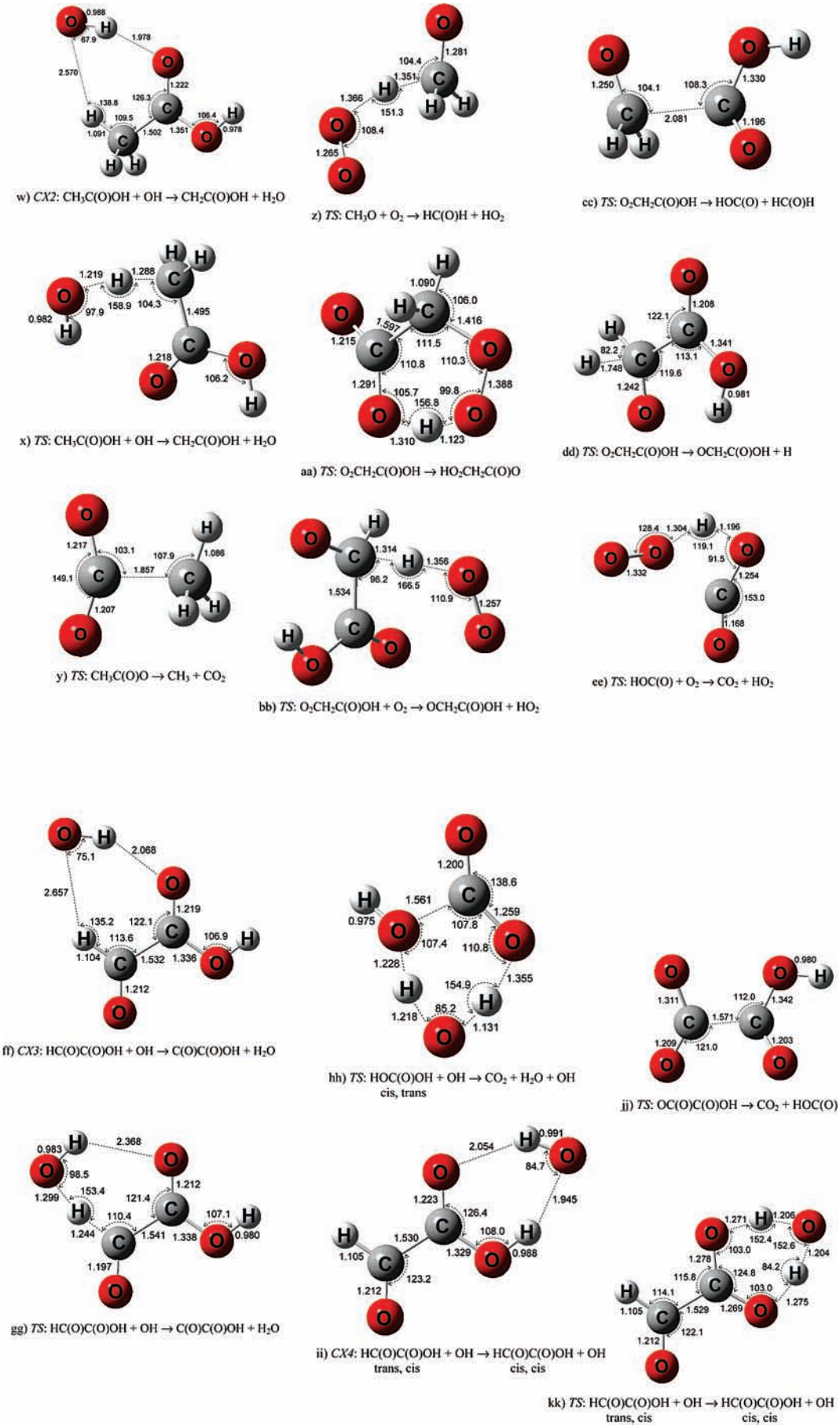

Figure 2. Geometries of closed- and open-shell species, prereactive complex, and transition state structures involved in the atmospheric oxidation of acetic acid. Parameters are calculated at the QCISD/6-31G(d) level of theory.

atoms becomes equivalent and symmetric. The breaking and forming OH bond lengths are 1.241 and 1.228 Å. Figure 2d shows the resulting cis,trans carbonic acid isomer.

The OH radical can also assist in the decomposition of the cis,trans conformer of carbonic acid (local minimum) into CO_2 and H_2O. The OH-assisted decomposition (Figure 2hh) involves the breaking of the OH bond on the trans side, which elongates by 0.361 Å. The OH radical also enlogates by 0.228 Å and the CO bond on the cis side by 0.200Å. A new bond 1.228 Å in length forms between the OH, ejecting on the cis side, and the H atom, from the dissociation of the initial OH radical. The OH-assisted decomposition is analogous to the reaction of CO_2 with water dimer, initially proposed by Jönsson et al.,[58−60] and latter pursued by Nguyen and co-workers.[61,62] The reaction proceeds via a six-member ring complex and transition state, with substantial ring deformation.

Pathway 2. Hydrogen abstraction from acetic acid at the carboxylic acid side yields the $CH_3C(O)O$ radical (Figure 1). The OCO angle decreases by 8.1° while the two CO bonds acquire a partial double bound character with lengths of 1.250 and 1.288 Å, after the release of the hydrogen atom. The abstraction of the acidic hydrogen involves a prereactive complex and a transition state. The complex structure is stabilized by hydrogen bonding, with values of 1.931 and 1.941 Å. The OH radical is aligned with the carbonyl oxygen and acidic hydrogen in a six-member-ring coplanar arrangement. In the transition state structure the OH radical H-atom orients itself out-of-plane with respect to the ring configuration. During the removal of the acidic hydrogen, the transition state structure is characterized by a five-member ring with a dihedral angle OOHO of 8.166°. Also the two CO bonds lengths become 1.274 and 1.275 Å. The product of the acid hydrogen abstraction, $CH_3C(O)O$ radical, decomposes to produce the CH_3 radical and CO_2. The transition state for this decomposition is shown in Figure 2y. It is clear that this transition leads to the formation of CO_2, where the OCO angle increases from 114.3° to 144.3°, and the CC bond elongates from 1.499 to 1.857 Å. In the troposphere, where the O_2 concentrations are on the order of 5×10^{18} molecules cm^{-3}, O_2 binds to alkyl radicals, such as CH_3, to produce, in this case, the methyl peroxy radical. In urban environments, NO abstracts O atoms from peroxy radicals to produce alkoxy radicals, shown in Figure 2g. The formation of ketones and aldehydes from alkoxy radicals takes place via H-abstraction by O_2. The transition state for the production of formaldehyde from methyl alkoxy radical is shown in Figure 2z. The O_2 molecule, with a bond length of 1.265 Å, is aligned trans with respect to the CO bond on the alkoxy radical. The forming O−H bond leading to the production of HO_2 has a length of 1.366 Å, while the breaking C−H bond has a length of 1.351 Å. The partial CO double bond length of the forming CH_2O molecule is 1.281 Å.

Pathway 3. Pathway 3 involves the abstraction of the methyl hydrogen from acetic acid by OH radicals (Figure 1). This pathway is also characterized by a stable complex and a transition state. The prereactive complex is stabilized by a looser hydrogen bond of 2.57 Å on the methyl side and a second hydrogen bond of 1.978 Å on the carbonyl side, in a six-member-ring configuration. The OH radical is aligned nearly planar with acetic acid, in a dihedral angle OHOH of 0.017°. During the transition from reactants to products, the H-atom being abstracted is out-of-plane ($\tau = 44°$) with respect to the carbonyl oxygen, leaving the remaining two H atoms in more of an in-plane position with respect to the carbonyl oxygen ($\tau = 160.9°$, 67.2°) with bond lengths of 1.090 and 1.092 Å. Hydrogen abstraction from acetic acid at the methyl side results in the formation of the $CH_2C(O)OH$ radical. Under typical atmospheric conditions, $O_2CH_2C(O)OH$ is formed from the reaction of $CH_2C(O)OH + O_2$. The structure of this peroxy radical is depicted in Figure 2i, characterized by the OCCO backbone atoms in *the cis* configuration ($\tau = 30.2°$) and the peroxy terminal in the trans configuration with respect to the CC bond. The peroxy radical can react in a variety of ways: it can rearrange internally or it can be reduced by NO under typical urban atmospheric conditions. During isomerization, both CO bonds rotate to accommodate the acidic hydrogen and the terminal peroxy atom into a six-member ring to facilitate the transference of the acidic hydrogen from the carboxylic acid side to the peroxy terminal. The geometry parameters of the peroxy isomerization transition state are depicted in Figure 2aa. Once in the six-member arrangement, the breaking OH bond increases by 25% while the HO bond on the peroxy side has a bond length of 1.123 Å. The peroxy OO bond increases from 1.345 to 1.388 Å to accommodate the previously acidic H atom into a new hydroperoxy bond. The acidic hydrogen atom is transferred between the two oxygen atoms in a OHO angle of 156.8°. The resulting hydroperoxy radical is expected to break apart into OH, CO_2, and HC(O)H.

Removal of the alkoxy ($OCH_2C(O)OH$) radical (Figure 2j) can take place via three different pathways: hydrogen ejection, reaction with O_2, and internal dissociation. Two of the branches, hydrogen ejection and reaction with O_2, lead to the formation of glyoxylic acid (HC(O)C(O)OH) while internal dissociation produces HC(O)H and HOC(O). The alkoxy radical is stabilized by a hydrogen bond. The transition state of its decomposition involves the internal rotation of the CO bond (1.346 Å in length) from the trans to the cis configuration prior to dissociation. The cis configuration makes the radical unstable and reactive enough to break apart and produce formaldehyde and *cis*-HOC(O). During decomposition, the CC bond length increases from 1.531 to 2.081 Å and the CO bond length on the formaldehyde-like side of the transition state decreases from 1.386 to 1.250 Å. Figure 2dd shows the transition state structure for the H-ejection pathway. The hydrogen atom is released from the alkoxy radical with a bond length of 1.748 Å. The former has a structure similar to the transition state for the reaction with O_2. The oxygen molecule is aligned in-plane with the CC bond. The H atom is abstracted from the C atom with a bond length of 1.314 Å, while making a new bond with O_2 1.356 Å in length to produce HO_2.

The main product of the alkoxy ($OCH_2C(O)OH$) chemistry is glyoxylic acid [HC(O)C(O)OH]. The structures of two glyoxylic acid isomers were analyzed in terms of their stability. The geometries of *trans*-(C(O)C(O))-*trans*-(C(O)OH) and *trans*-(C(O)C(O))-*cis*-(C(O)OH) were shown to be almost identical in stability, with a very small CO bond rotational energy of less than 0.01 kcal/mol. It is then expected that both isomers will exist in equilibrium. For practical purposes we will refer to the trans-cis configuration in discussing its atmospheric degradation. The removal of the terminal H atom is also characterized by a prereactive complex and transition state, in Figures 2ff and 2gg, respectively. In the complex structure the OH radical is aligned in-plane with glyoxylic acid, stabilizing it with a single hydrogen bond of 2.068 Å into a six-member ring configuration. In the transition state structure the OH radical abstracts the terminal hydrogen with a bond length of 1.299 Å, where the CH bond extends from 1.104 to 1.244 Å. This reaction results in the formation of the C(O)C(O)OH radical. The previous C(O)−C(O) bond, aligned trans with respect of each other, now bends out-of-plane with a dihedral angle of 83.8°.

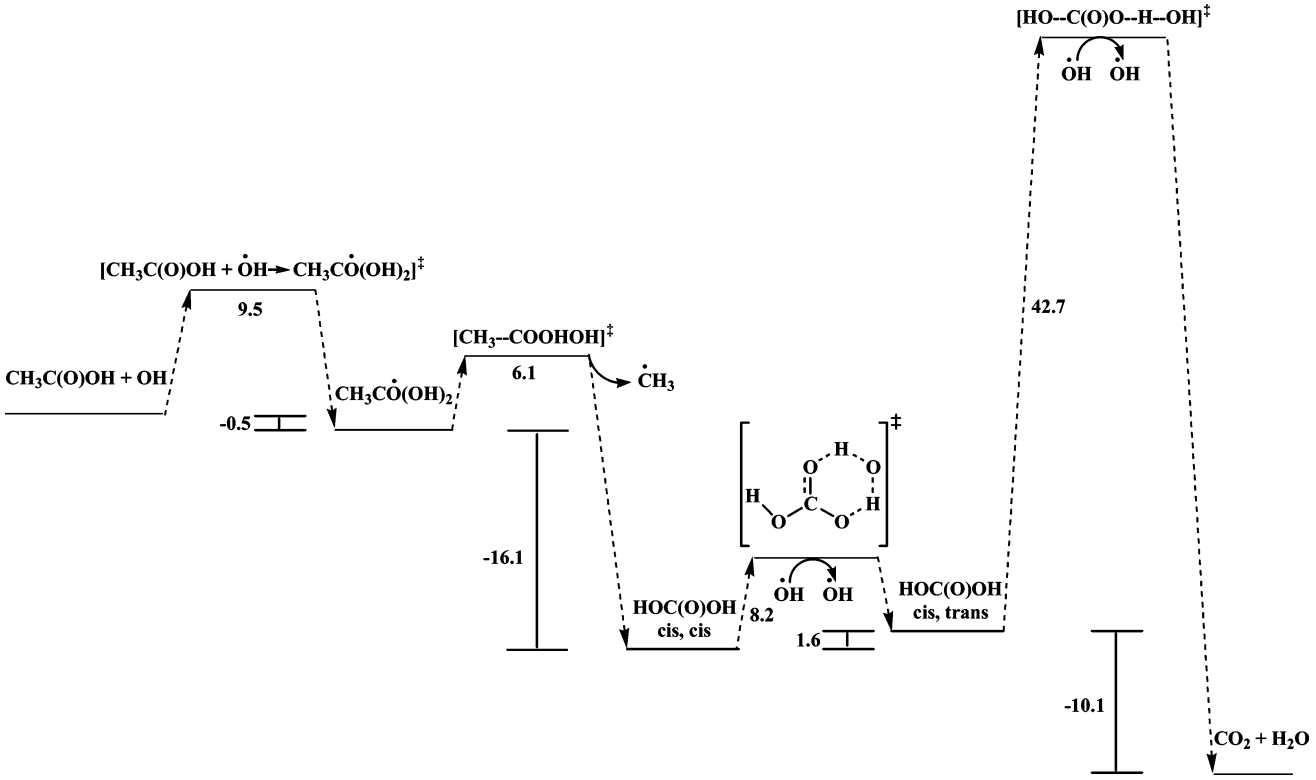

Figure 3. Pathway 1.

An O_2 molecule attaches to the vacant out-of-plane radical site on C(O)C(O)OH, forming $O_2C(O)C(O)OH$ (Figure 2n). The formed peroxide C−O_2 bond has a bond length of 1.398 Å, while the terminal OO bond lengthens to 1.355 Å. The O_2C-(O)C(O)OH radical is reduced to OC(O)C(O)OH by NO. Stabilization by hydrogen bonding seems to be relevant for the peroxy radical. The carboxylic acid side is arranged in a trans configuration to facilitate a hydrogen bond interaction of 2.163 Å between the terminal hydrogen and the oxygen atom of the second carbonyl group (1.201 Å). On the other hand, after the peroxy radical is reduced the arrangement of the carboxylic acid terminal switches from trans to cis. The alkoxy radical is expected to decompose into CO_2 and HOC(O). The transition state for the alkoxy decomposition (Figure 2jj) is characterized by the elongation of the CC bond by 3%, and a rotation along the CC axis, switching from a coplanar to an asymmetric structure with a dihedral angle of 34.9°.

As previously observed during the degradation of carbonic acid, OH radicals can facilitate the isomerization of glyoxylic acid from the trans,cis to the cis,cis configuration. The reaction of glyoxylic acid with OH radicals on the carboxylic acid terminal involves the formation of a strongly bonded prereactive complex with hydrogen bonds of 2.054 and 1.945 Å. The reaction is characterized by a transition state where an OH radical assists the isomerization by transferring its hydrogen atom to the carbonyl oxygen while abstracting the terminal acidic hydrogen, as shown in Figure 2kk. The transference takes place by the equal sharing of the hydrogen atoms in a six-member-ring configuration. The single and double CO bonds have partial double bond characteristics with bond lengths of 1.269 and 1.278 Å, the carboxylic OH breaking and forming bonds have bond lengths of 1.275 and 1.271 Å, and the transitioning OH radical bonds exchange the hydrogen atoms around the ring configuration with closely equivalent bond lengths of 1.204 and 1.206 Å. Figure 2p shows the cis,cis glyoxylic acid isomer, where both carbonyl groups are oriented cis with respect to one another with bond lengths of 1.212 and 1.208 Å, and the CO and OH bonds on the carboxylic side are also oriented cis.

B. Energetics of the Potential Energy Surface. The potential energy surface of pathway 1 is depicted in Figure 3. The addition of the OH radical to the central carbon atom on the C═O bond on acetic acid produces the $CH_3CO(OH)_2$ radical intermediate. The enthalpy of reaction is predicted to be −0.5 kcal/mol at the QCISD(T)/6-31++G(2d,2p) level of theory, and −0.5 kcal/mol with the QCISD(T)/6-31++G(2df,2p) level of theory. The ab initio calculations predicted an energy barrier for the OH addition to the C═O bond in acetic acid of 8.2 and 9.5 kcal/mol at the QCISD(T)/6-31++G(2d,2p) and QCISD(T)/6-31++G(2df,2p) levels of theory, respectively. The transition state vibrational frequency analysis indicates that it is a first-order saddle point characterized by one negative frequency of −740 cm^{-1}. Previous theoretical studies by De Smedt et al.[45] of the potential energy surface of the $CH_3C(O)OH$ + OH reaction predicted an energy barrier of 9.5 kcal/mol and a heat of reaction of −0.8 kcal/mol by using G2M(CC,MP2)//B3LYP/6-311++G(2df,2pd) levels of theory. The energetics of our ab initio study and those previously determined by De Smedt and co-workers[45] differ by approximately 0.3 kcal/mol on the heat of reaction. The OH addition channel has been explored as a potential pathway during previous investigations on the reaction of the OH radical with aldehydes and ketones.[35,35,49,50] The addition of OH to the carbon atom of the C═O group was found to occur through a loosely bound complex, with similar structure to that of the transition state. In comparison with the hydrogen abstraction channels, the binding energy for the OH-addition prereactive complex was smaller, and the activation barriers were higher by ∼5−10 kcal/mol, making this channel kinetically unfavorable.

The produced $CH_3CO(OH)_2$ radical from the OH addition pathway then releases a methyl radical to form carbonic acid [HOC(O)OH] in the cis,cis conformation. Several investigations

have recognized the stability and relevance of carbonic acid in different matrixes and experimental conditions.[51−54] Carbonic acid is produced in nature from the hydration of carbon dioxide. This reaction is considered fundamental in biological and ecological systems.[55,56] Magid et al.[57] reported an activation barrier of 17.7 kcal/mol for the reaction of the hydration of carbon dioxide in a neutral solution

$$(CO_2)_{aq} + H_2O \leftrightarrow (H_2CO_3)_{aq} \leftrightarrow (HCO_3^-)_{aq} + (H^+)_{aq} \quad (20)$$

On the other hand, early computational studies with SCF calculations found that the gas-phase hydration of CO_2 proceeds with an activation barrier of 54.8 kcal/mol, [58−60] suggesting a large fundamental discrepancy in the reaction mechanism between the solution and the gas phase. A later study by Nguyen et al.[61] showed that the addition of at least a second water molecule has a significant catalytic effect, by participating as an intermediate in the proton transfer and lowering significantly the energy barrier, as observed in related water oligomer systems.[62] The transition state for the $CO_2 + H_2O$ reaction involves the proton transfer from a water molecule to one of the oxygen atoms of carbon dioxide, with a high energy barrier of 49.2 kcal/mol calculated by Nguyen et al.[61] This is comparable with 55.9 kcal/mol determined by Jönsson et al.,[59] and in the same order of magnitude as the values found for intramolecular 1,3-proton transfer reactions.[63] On the other hand, the reaction of $CO_2 + 2H_2O$ produces carbonic acid via a six-member cyclic complex with a binding energy of 24.1 kcal/mol, and an analogous transition state at 8.6 kcal/mol below $CO_2 + 2\ H_2O$. Wight et al.[48] revisited the energetics of the reaction of $CO_2 + H_2O$ (reaction 19) by performing ab initio calculations at MP2(full)/6-31++G(d,p)//QCISD(T)/6-311++G-(d,p) and determined energy barriers for the forward and reverse reactions of 51.9 and 41.5 kcal/mol, respectively. Loerting and co-workers[54] investigated the kinetic stability of carbonic acid by examining the influence of water molecules on its decomposition rate. The addition of two water molecules increased the rate of decomposition by 10 orders of magnitude at 300 K.

In our study we found that OH radicals could assist in the isomerization of carbonic acid as well as the decomposition of the cis,trans carbonic acid isomer. The energetics of these two reactions, calculated at QCISD(T)/6-31++G(2df,2p)//QCISD/6-31G(d), are presented in Figure 3. The OH-assisted intermolecular isomerization proceeds with an activation barrier of 8.2 kcal/mol and it is endothermic by 1.6 kcal/mol. Wight et al.[48] also examine the potential energy surface of the intramolecular conversion of cis,cis carbonic acid into its cis,trans isomer at QCISD(T)/6-311++G(d,p)//MP2(full)/6-31++G(d,p) levels of theory. The transition state involving the rotation along the C−O bond and the cis,trans isomer lie above cis,cis carbonic acid by 9.2 and 1.6 kcal/mol, respectively. Since the results reported by Wight et al.[48] are in accord with ours within 1 kcal/mol, OH radicals are not expected to participate as a catalyst in the isomerization reaction, but rather as a chaperon. The energy barriers are basically unchangeable with or without the participation of OH radicals. A similar phenomenon is observed during the decomposition of the carbonic acid isomer in the presence of OH radicals. As with the reaction of carbon dioxide with two water molecules, the transition state of the OH-assisted H_2-CO_3 decomposition involves a six-member cyclic transition state with a similar degree of ring deformation. On the other hand, the exothermicity and activation barrier of the decomposition of cis,trans carbonic acid in the presence of OH radicals depicted in Figure 3 (−10.1, 42.4 kcal/mol) and those obtained at CCSD-(T)/aug-cc-pVDZ//MP2/aug-cc-pVDZ///B3LYP/6-31+G(D) by Loerting et al.[54] for the decomposition of isolated carbonic acid are in very good agreement (−9.05, 43.55 kcal/mol). OH radicals do not have the same catalytic effect as water molecules in lowering the activation barriers of these types of chemical reactions. A possible explanation, as argued by Olkhov et al.,[64] for the difference in reactivity between carbonic acid with OH vs H_2O, being the reaction of $H_2CO_3 + H_2O$ faster, may rely on the fact that OH is an open shell and H_2O a closed shell system.

Pathway 2 consists of the abstraction of the acidic hydrogen from acetic acid by the OH radical. The energetics of pathway 2 has been explored in detail by De Smedt et al.[45] up to the decomposition of the alkyl radical. For completeness, with the goal of determining the final byproducts of the acetic acid atmospheric degradation, the chemistry of the methyl peroxy radical needs to be considered. In searching for the prereactive complex and transition state structures a six-member-ring prereactive complex and a five-center transition state were located, as previously suggested by De Smedt and co-workers,[45] who estimated a complex well −7.3 kcal/mol below and a transition state barrier 1.6 kcal/mol above the reactants level at G2M//B3LYP/6-311++G(2df,2p). In the present study, the prereactive complex binding energy is 6.5 kcal/mol, as shown in Table 2, and the activation barrier is 2.1 kcal/mol, as shown in Table 1, determined at the QCISD(T)/6-31++G(2df,2p)//QCISD/6-31G(d) level of theory. There is only one imaginary frequency attributed to this transition state structure with the value of 1648 cm^{-1}, indicating that the transition state is a first-order saddle point. De Smedt et al.[45] found a discrepancy of 1.7 kcal/mol on the predicted barrier height values for this transition state structure between the G2M//MP2/6-311++G-(2df,2p) and G2M//B3LYP/6-311++G(2df,2p) levels, and concluded that the values from the B3LYP method underestimated the barrier height while those from the MP2 method overestimate it. Our predicted barrier height value lies between those determined by De Smedt and co-workers[45] Hydrogen abstraction at the acidic C(O)OH terminal results in the formation of the $CH_3C(O)O$ radical, which may decompose into CO_2 and the CH_3 radical. This decomposition reaction is characterized by a negative energy barrier and a large exothermicity of −22.7 kcal/mol. Methyl peroxy radicals are produced from the addition of O_2 to the vacant radical site on the methyl radical. O_2 can also participate in the abstraction reaction where it removes a hydrogen atom from methoxy radicals to form formaldehyde and HO_2. The reaction is very exothermic, having a reaction enthalpy of −26.3 kcal/mol. The activation energy barrier is also large with a value of 17.0 kcal/mol.

A detailed schematic description of the potential energy surface of pathway 3 is shown in Figure 5A,B. Pathway 3 consists of the direct abstraction of a methyl hydrogen from acetic acid by OH radicals. The reaction of $CH_3C(O)OH + OH$ going to $CH_2C(O)OH + H_2O$ is exothermic by −17.8 kcal/mol at the QCISD(T)/6-31++G(2df,2p)//QCISD/6-31G(d) level. The activation energy barrier is estimated to be 4.0 kcal/mol and the prereactive complex has a binding energy of 4.4 kcal/mol. The transition state for this reaction is a first-order saddle point with an imaginary frequency at 2265*i* cm^{-1}. De Smedt and co-workers[45] proposed that the prereactive complex and transition state of this reaction lie 5.1 kcal/mol below and 4.0 kcal/mol above the $CH_3C(O)OH + OH$ reactant level, respectively. Even though the energy barrier predicted in this study and that reported by De Smedt and co-workers[45] are the same, the nature of the transition state structures responsible for those energy barriers is different. Figure 2x shows the transition state

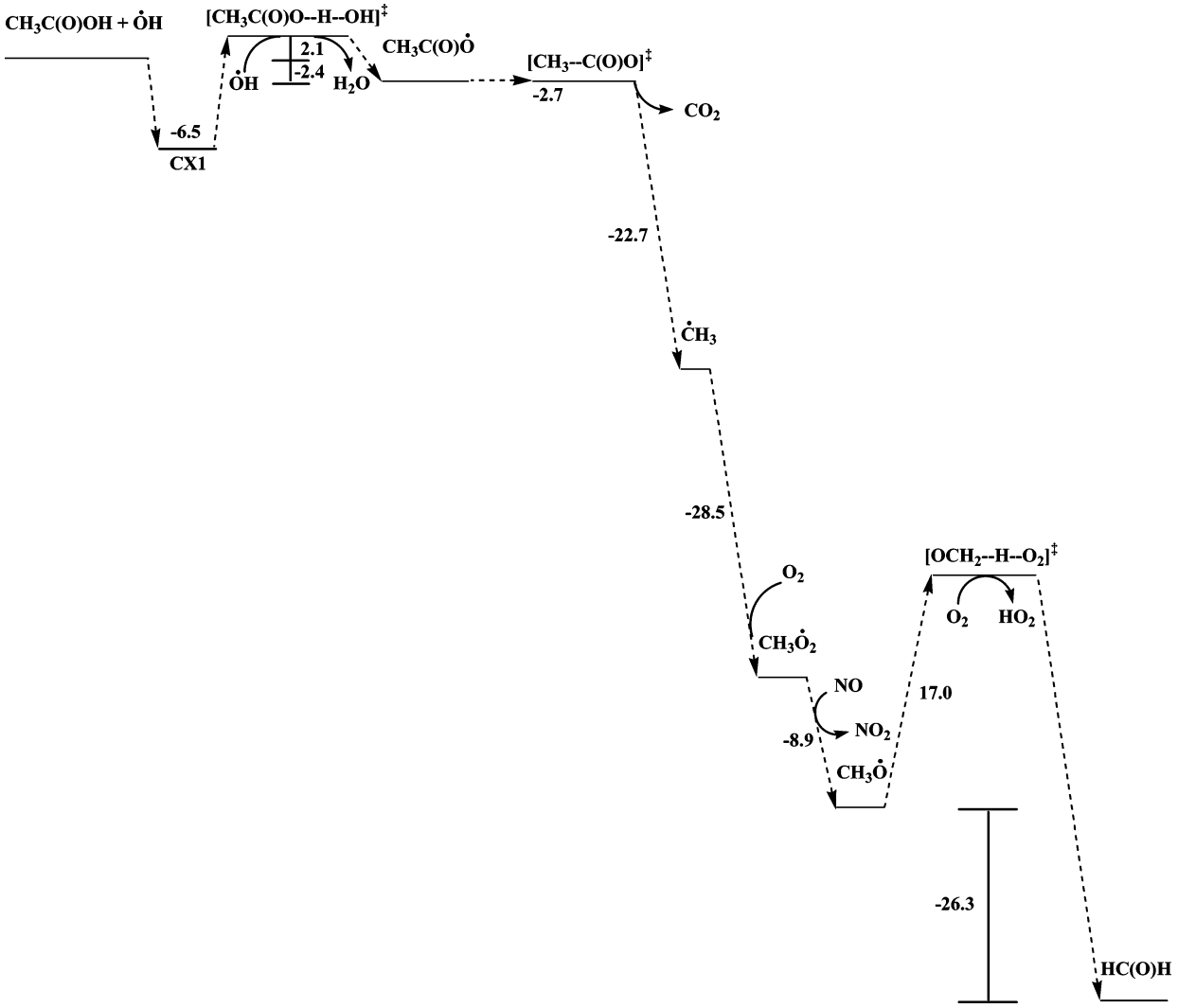

Figure 4. Pathway 2.

structure predicted in this study. The structure still resembles the six-member hydrogen bonded nature of the prereactive complex. The corresponding structure suggested by De Smedt and co-workers[45] lacks hydrogen bonding character.

As part of the comprehensiveness of this study, the chemistry of $O_2CH_2C(O)OH$ has been examined, which will enable us to predict the final product from the acetic acid atmospheric degradation. The $O_2CH_2C(O)OH$ radical is produced as the result of the O_2 addition to the radical site on the $CH_2C(O)OH$ radical. Two different reaction channels for $O_2CH_2C(O)OH$ are considered. The first is its intramolecular isomerization and further decomposition and the second is its reduction by NO. The isomerization pathway is endothermic by 26.0 kcal/mol, as it passes through a barrier of 26.4 kcal/mol. The isomerization of the peroxy radical is not expected to play a major role in the degradation mechanism. However, the reaction with NO forming $OCH_2C(O)OH$ and NO_2 is expected to be the main reaction channel, which is thermodynamically favored by −8.9 kcal/mol. Under atmospheric conditions, NO is found in much larger concentrations than peroxy radicals. Therefore, the reaction of peroxy radicals with NO will dominate over the self-reaction.[65,66] The alkoxy radical $OCH_2C(O)OH$ may react by three different means

$$OCH_2C(O)OH \rightarrow HC(O)C(O)OH + H \quad (21)$$

$$OCH_2C(O)OH \rightarrow HC(O)H + HOC(O) \quad (22)$$

$$OCH_2C(O)OH + O_2 \rightarrow HC(O)C(O)OH + HO_2 \quad (23)$$

Reaction 21 consists of hydrogen atom ejection that produces glyoxylic acid. The reaction is endothermic, with a reaction enthalpy of 11.9 kcal/mol, and has an activation barrier of 17.0 kcal/mol. Reaction 22 is a unimolecular CC bond fission reaction, producing formaldehyde and the HOC(O) radical, over a barrier height of 10.0 kcal/mol and an enthalpy of −3.8 kcal/mol. Although the $OCH_2C(O)OH$ structure in Figure 2j is the global minimum, it must rotate along the carboxylic CO bond into a dihedral angle of 0.0 before it can access the bond fission reaction pathway. Reaction 23 is an abstraction reaction in which O_2 abstracts a hydrogen atom to form glyoxylic acid and HO_2. The reaction is very exothermic, having a reaction enthalpy of −33.4 kcal/mol and a rather small activation energy barrier of 6.1 kcal/mol. Among all possible pathways, the O_2 reaction is the most kinetically favored pathway.

Even though the reaction with O_2 is the most accessible, a small fraction of $OCH_2C(O)OH$ radicals will dissociate into formaldehyde and HOC(O). HOC(O) is of relevance in the atmosphere because it is a relatively stable radical. The reaction of HOC(O) with O_2 has been examined in detail by Poggi and Francisco.[67] Among the pathways examined, only the direct hydrogen abstraction by O_2 forming HO_2 and CO_2 is considered

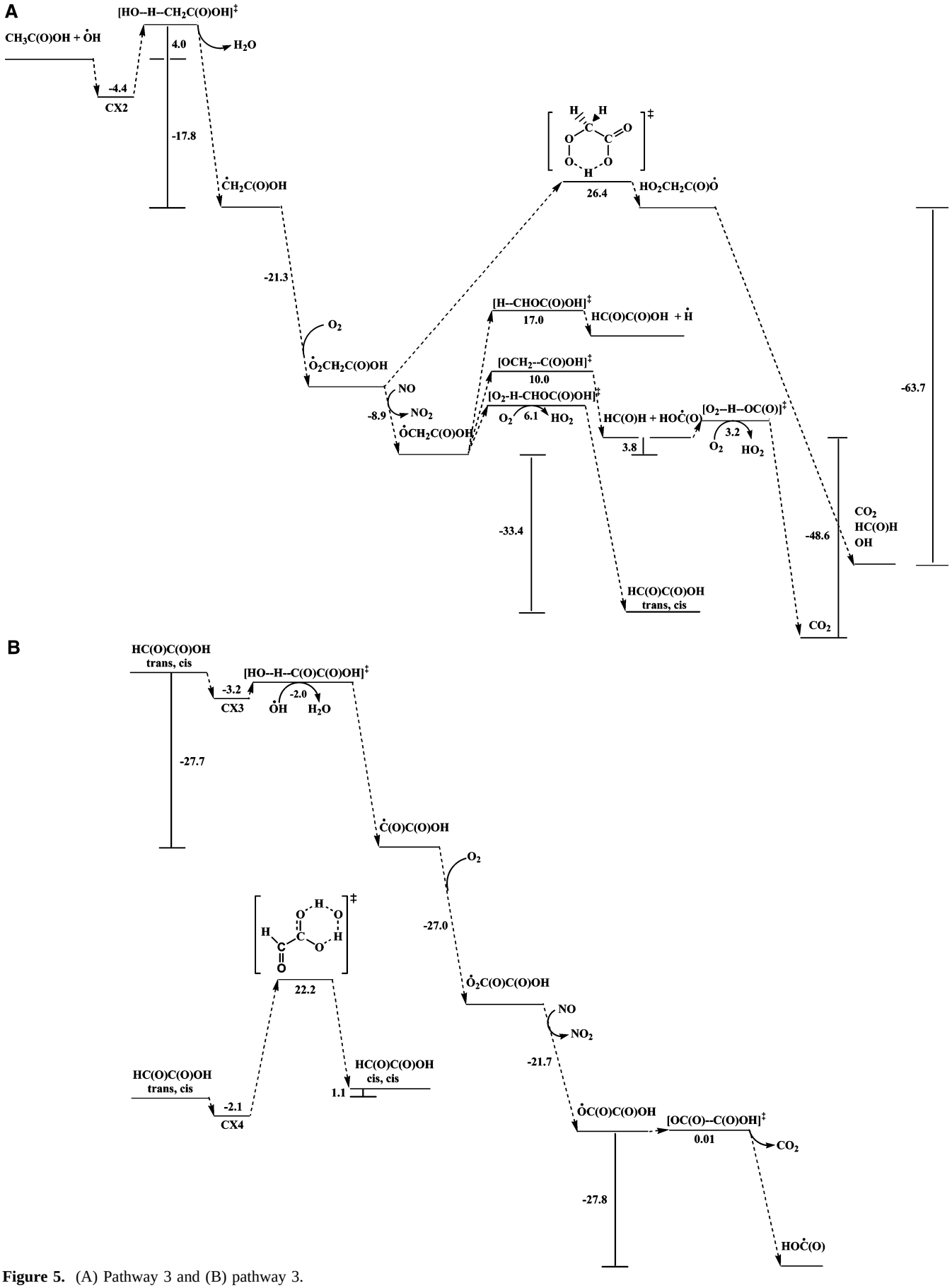

Figure 5. (A) Pathway 3 and (B) pathway 3.

in this study. The reaction is very exothermic by −48.6 kcal/mol and has a small barrier height of 3.2 kcal/mol at QCISD-(T)/6-31++G(2df,2p) levels of theory. Our results are in very good agreement within 0.4 kcal/mol with those obtained by

Poggi et al.[67] determined 0.4 kcal/mol at QCISD(T)/6-311++G-(3df,3pd)//QCISD/6-31G(d).

It has been demonstrated that glyoxilic acid [HC(O)C(O)-OH] is a major byproduct from the atmospheric degradation of acetic acid through pathway 3. Glyoxylic acid has been identified and measured in the atmosphere aqueous phase (rain, mist, fog).[68−70] Presently, the sources of dicarboxylic acids in fog and mist are not known. Also, because of their lower vapor pressure compared to that of monocarboxylic acids, dicarboxylic acids are expected to be found predominantly in particles. The importance of heterogeneous chemistry within aerosol surfaces and cloud droplets has been addressed as a potential pathway for their presence in particulate matter, by either the uptaking of acids in the gas phase or the formation within cloud droplets and particles. The role of dicarboxylic acids in the atmosphere is not known.

This theoretical study contains the first data on the prediction of the atmospheric fate of glyoxilic acid. Figure 5B shows the relevant energetics for the atmospheric degradation mechanism of glyoxylic acid. The hydrogen abstraction reaction of glyoxilic acid with OH radicals on the carbonyl side proceeds with the formation of a loosely bonded prereactive complex, which has a small binding energy of −3.2 kcal/mol. The transtition state structure lays −2.0 kcal/mol below the reactants level. The slight negative activation energy barrier should result in a non-Arrhenius behavior where the prereactive complex is expected to be in equilibrium with the reactants and the reaction rate constant of the HC(O)C(O)OH + OH reaction decreases as the temperature increases. The reaction is irreversible due to a large heat of reaction of −27.7 kcal/mol.

The C(O)C(O)OH radical results from the removal of the carbonyl hydrogen in glyoxylic acid by the OH radical. O_2 binds to the C(O)C(O)OH vacant radical site to form $O_2C(O)C(O)$-OH, with a heat of formation of −27.0 kcal/mol, typical for peroxy radicals. Under atmospheric conditions, the reaction with NO to produce the alkoxy radical, OC(O)C(O)OH, and NO_2 is exothermic by −21.7 kcal/mol. The alkoxy radical is expected to break apart into CO_2 and HOC(O). The reaction is barrierless with an almost negligible barrier height of 0.01 kcal/mol, even though one imaginary frequency of 814*i* cm^{-1} was found in the transition state structure. On the acidic side, the OH radical assists in the isomerization reaction of trans,cis glyoxilic acid into the cis,cis conformer (Figure 2p), as previously observed with carbonic acid. The OH-mediated intermolecular isomerization of glyoxylic acid proceeds with an activation barrier of 22.2 kcal/mol and it is slightly endothermic by 1.1 kcal/mol. The transition state structure is a first-order saddle point characterized by one imaginary frequency at 1892*i* cm^{-1}. The formation of a loose complex with a binding energy of 2.1 kcal/mol precedes the transition state. Since the two glyoxylic acid isomers differ in energy by only ∼1.0 kcal/mol, it is expected that glyoxylic acid will exist in both conformations even though the interconversion between both will be slow.

Atmospheric Implications

Ab initio molecular orbital calculations have been carried out to investigate the potential energy surface for the $CH_3C(O)OH$ + OH reaction. The analysis of energetics and vibrational frequencies allowed us to depict the major features of the atmospheric oxidation mechanism. The prediction of major byproducts from the oxidation chemistry is crucial to determine the role played by acetic acid in the atmosphere. The reaction mechanism explored in this study consists of three pathways: (1) OH addition to the carbon atom of the central C═O bond, (2) abstraction of the methyl hydrogen, and (3) abstraction of the acidic hydrogen. The major products from each pathway have been predicted. The OH-addition channel (pathway 1) results in the production of carbonic acid on its cis,cis conformation. For the first time it has been revealed that OH radicals can assist as intermediates on isomerization reactions. This is the case for the isomerization of carbonic acid from the cis,cis to the cis,trans conformation, where OH radical participates on the 1,3 proton-transfer reactions. It was found that OH also assists on the decomposition of the cis,trans carbonic acid conformer without the catalytic effect that water has when it is added during the decomposition of carbonic acid.

The abstraction of the acidic hydrogen (pathway 2) leads to the production of methyl radicals, followed by the addition of O_2 to form methyl peroxy radicals, from which formaldehyde and HO_2 are obtained as major products. Formaldehyde leads to an additional source of HO_2 in its oxidation to CO. As a consequence of pathway 2 this route should result in an increase of atmospheric HO_x.

The third pathway involves the removal of a methyl hydrogen to form $CH_2C(O)OH$. The incorporation and examination of the peroxy radical chemistry is essential in determining the final products in this study. The peroxy radical, $O_2CH_2C(O)OH$, is formed from the O_2 addition to the vacant radical site on CH_2C-(O)OH. Through the formation of the alkoxy radical, the ultimate fate of the peroxy radical is the formation of HOC(O) and glyoxylic acid. HOC(O) has been found to be a stable radical intermediate. A lifetime of ∼1 ms has been previously estimated for HOC(O). Under atmospheric conditions of ∼20% O_2, it is expected that the main HOC(O) removal mechanism would be reaction with O_2, leading to CO_2 and HO_2.

The atmospheric degradation chemistry of glyoxilic acid has been explored in detail for the first time in this study. Little is known of the role played by dicarboxylic acids in the atmosphere. The removal of the terminal hydrogen is characterized by the formation of prereactive complexes and negative activation barriers. This has important implications for the atmospheric lifetime of glyoxylic acid. The lifetime of glyoxilic acid toward OH removal is expected to increase in the upper troposphere and lower stratosphere.

The present calculations suggest that the kinetics of the acetic acid degradation reaction mechanism are going to be strongly influenced by complex-forming routes. A major finding from this study is the participation of the OH radical in mediating isomerization and decomposition reactions. This was the case for the isomerization and decomposition of carbonic acid and the isomerization of glyoxilic acid. This type of interaction took place during the OH radical reaction at the carboxylic acid terminal in these molecules.

Conclusion

The energetics of the atmospheric degradation mechanism of acetic acid initiated by OH radicals have been explored in detail. The reaction of $CH_3C(O)OH$ + OH will proceed mainly via the abstraction of acidic hydrogen (pathway 2). Hydrogen abstraction takes place via the formation of a prereactive complex, with binding energy of 6.5 kcal/mol, and a transition state structure with a 2.1 kcal/mol energy barrier. The main products from each of the three reaction pathways have been identified; pathway 1 leads to the production of carbonic acid, pathway 2 generates formaldehyde, and pathway 3 will primarily produce glyoxylic acid through the reaction of the alkoxy radical, $OCH_2C(O)OH$, with O_2. Formaldehyde also reacts with hydroxyl radicals to form HO_2 and CO. The fate of glyoxylic

acid in the atmosphere has been explored. The atmospheric degradation chemistry of glyoxylic acid is responsible for the formation of HOC(O), which will in turn be converted into CO_2 and HO_2.

This study showed unique OH-mediated isomerization and decomposition reactions. This was the case for the isomerization and decomposition of carbonic acid and isomerization of glyoxylic acid, both taking place at the carboxylic acid side.

These results will provide insights for future studies in determining overall reaction rate constants at a wide range of temperature and pressure conditions as well as in reproducing acetic acid concentrations in global 3-D atmospheric reactivity models.

Supporting Information Available: Tables of calculated total energies for products, prereactive complexes, reactants, and transition states for species involved in the acetic acid oxidation and vibrational frequencies for all species calculated at the QCISD/6-31G(d) level of theory. This material is available free of charge via the Internet at http://pubs.acs.org.

References and Notes

(1) Chebbi, A.; Carlier, P. *Atmos. Environ.* **1996**, *30*, 4233.

(2) Khare, P.; Kumar, N.; Kumari, K. M.; Srivastava, S. S. *Rev. Geophys.* **1999**, *37*, 227.

(3) Grosjean, D. *Environ. Sci. Technol.* **1989**, *23*, 1506.

(4) Talbot, R. W.; Mosher, B. W.; Heikes, B. G.; Jacob, D. J.; Munger, B. C.; Daube, B. C.; Keene, W. C.; Maben, J. R.; Artz, R. S. *J. Geophys. Res.* **1995**, *100*, 9335.

(5) Keene, W. C.; Mosher, B. W.; Jacob, D. J.; Munger, J. W.; Talbot, R. W.; Artz, R. S.; Maben, J. R.; Daube, B. C.; Galloway, J. N. *J. Geophys. Res.* **1986**, *91*, 14466.

(6) Sanhueza, E.; Figueroa, L.; Santana, M. *Atmos. Environ.* **1996**, *30*, 1861.

(7) Granby, K.; Christensen, C. S.; Lohse, C. *Atmos. Environ.* **1997**, *31*, 1403.

(8) Granby, K.; Egeløv, A. H.; Nielsen, T.; Lohse, C. *J. Atmos. Chem.* **1997**, *28*, 195.

(9) Helas, G.; Bingemer, H.; Andreae, M. O. *J. Geophys. Res.* **1992**, *97*, 6187.

(10) Arlander, D. W.; Cronn, D. R.; Farmer, J. C.; Menzia, F. A.; Farmer, H. H. *J. Geophys. Res.* **1990**, *95*, 16391.

(11) Chapman, E. G.; Kenny, D. V.; Busness, K. M.; Thorp, J. M.; Spicer, C. W. *Geophys. Res. Lett.* **1995**, *22*, 405.

(12) Talbot, R. W.; Andreae, M. O.; Berresheim, H.; Jacob, D. J.; Beecher, K. M. *J. Geophys. Res.* **1990**, *93*, 1638.

(13) Gregory G. L. *J. Geophys. Res.* **1986**, *91*, 8603.

(14) Khwaja, H. A. *Atmos. Environ.* **1995**, *29*, 127.

(15) Talbot, R. W.; Beecher, K. M.; Harris, R. C.; Cofer, W. R. *J. Geophys. Res.* **1988**, *93*, 1638.

(16) Andreae, M. O.; Talbot, R. W.; Andreae, T. W.; Harris, R. C. *J. Geophys. Res.* **1988**, *93*, 1616.

(17) Kawamura, K.; Ng, L.; Kaplan, I. R. *Environ. Sci. Technol.* **1985**, *19*, 1082.

(18) Enders, G.; Dlugi, R.; Steincrecher, R.; Clement, B.; Daiber, R.; Eijik, J. V.; Gab, S.; Haziza, M.; Helas, G.; Hermann, U.; Kessel, M.; Kesselmeier, J.; Kotzias, D.; Kourtidis, K.; Kurth, H. H.; McMillen, R. T.; Roider, G.; Schurmann, W.; Teichmann, U.; Torres, L. *Atmos. Environ.* **1992**, *26*, 171.

(19) Keene, W. C.; Galloway, J. N. *Tellus, Ser. B* **1988**, *40*, 322.

(20) Talbot, R. W.; Andreae, M. O.; Berresein, H.; Jacob, D. J.; Beecher, K. M. *J. Geophys. Res.* **1990**, *95*, 16799.

(21) Servant, J.; Kouadio, G.; Cros, B.; Delmas, R. *J. Atmos. Chem.* **1991**, 12, 367.

(22) Kesselmeier, J.; Bode, K.; Hofmann, U.; Müller, H.; Schäfer, L.; Wolf, A.; Ciccioli, P.; Brancaleoni, E.; Cecinato, A.; Frattoni, M.; Foster, P.; Ferrari, C.; Jacob, V.; Fugit, J. L.; Dutaur, L.; Simon, V.; Torres, L. *Atmos. Environ.* **1997**, *31* (SI), 119.

(23) Kesselmeier, J.; Staudt, M. *J. Atmos. Chem.* **1999**, *33*, 23.

(24) Staudt, M.; Wolf, A.; Kesselmeier, J. *Biogeochemistry* **2000**, *48* (2), 199.

(25) Rozyckit, H.; Strzelczyk E. *Plant. Soil.* **1986**, *96*, 337.

(26) Moortgat, G. K.; Veyret, B.; Lesclaux, R. *J. Phys. Chem.* **1989**, *93*, 2362.

(27) Niki, H.; Maker, P. D.; Savage, C. M.; Breitenbach, L. P. *J. Phys. Chem.* **1985**, *89*, 588.

(28) Moortgat, G. K.; Veyret, B.; Lesclaux, R. *Chem. Phys. Lett.* **1989**, 160, 443.

(29) Madronich, S.; Calvert, J. G. *J. Geophys. Res.* **1990**, *95* (D5), 5697.

(30) Kenley, R. A.; Traylor, T. G. *J. Am. Chem. Soc.* **1975**, *97*, 4700.

(31) Madronich, S.; Chatfield, R. B.; Calvert, J. G.; Moortgat, G. K.; Veyret, B.; Lesclaux, R. *Geophys. Res. Lett.* **1990**, *17* (12), 2361.

(32) Wollenhaupt, M.; Carl, S. A.; Horowitz, A.; Crowley, J. N. *J. Phys. Chem. A* **2000**, *104*, 2695.

(33) Wollenhaupt, M.; Crowley, J. N. *J. Phys. Chem. A* **2000**, *104*, 6429.

(34) Vasvári, G.; Szilágyi, I.; Bencsura, Á.; Dóbé, S.; Bérces, T.; Henon, E.; Canneaux, S.; Bohr, F. *Phys. Chem. Chem. Phys.* **2001**, *3*, 551.

(35) Vandenberk, S.; Vereecken, L.; Peeters, J. *Phys. Chem. Chem. Phys.* **2002**, *4*, 461.

(36) Wine, P. H.; Astalos, R. J.; Mauldin, R. L., III *J. Phys. Chem.* **1985**, *89*, 2620.

(37) Jolly, G. S.; McKenney, D. J.; Singleton, D. L.; Paraskevopoulos, G.; Bossard, A. R. *J. Phys. Chem.* **1986**, *90*, 6557.

(38) Singleton, D. L.; Paraskevopoulos, G.; Irwin, R. S.; Jolly, G. S.; McKenney, D. J. *J. Am. Chem. Soc.* **1988**, *110*, 7786.

(39) Galano, A.; Alvarez-Idaboy, J. R.; Ruiz-Santoyo, Ma. E.; Vivier-Bunge, A. *J. Phys. Chem. A* **2004**, *106*, 9520.

(40) Kuhlmann, R.; Lawrence, M. G.; Crutzen, P. J. *J. Geophys. Res.* **2003**, *108* (D23), 4729.

(41) Singh, H.; Chem, Y.; Tabazadeh, A.; Fukui, Y.; Bey, I.; Yantosca, R.; Jacob, D.; Arnold, F.; Wohlfrom, K.; Atlas, E.; Flocke, F.; Blake, D.; Blake, N.; Heikes, B.; Snow, J.; Talbot, R.; Gregory, G.; Sachse, G.; Vay, S.; Kondo, Y. *J. Geophys. Res.* **2000**, *105* (D3), 3795.

(42) Dagaut, P.; Wallington, T. J.; Liu, R.; Kurylo, M. *Int. J. Chem. Kinet.* **1988**, *20*, 331.

(43) Singleton, D. L.; Paraskevopoulos, G.; Irwin, R. S. *J. Am. Chem. Soc.* **1989**, *111*, 5248.

(44) Butkovskaya, N. I.; Kukui, A.; Pouvesle, N.; Le Bras, G. *J. Phys. Chem. A* **2004**, *108*, 7021.

(45) De Smedt, F.; Bui, X. V.; Nguyen, T. L.; Peeters, J.; Vereecken, L. *J. Phys. Chem. A* **2005**, *109*, 2401.

(46) Frisch, M. J.; Trucks, G. W.; Schlegel, H. B.; Scuseria, G. E.; Robb, M. A.; Cheeseman, J. R.; Montgomery, J. A., Jr.; Vreven, T.; Kudin, K. N.; Burant, J. C.; Millam, J. M.; Iyengar, S. S.; Tomasi, J.; Barone, V.; Mennucci, B.; Cossi, M.; Scalmani, G.; Rega, N.; Petersson, G. A.; Nakatsuji, H.; Hada, M.; Ehara, M.; Toyota, K.; Fukuda, R.; Hasegawa, J.; Ishida, M.; Nakajima, T.; Honda, Y.; Kitao, O.; Nakai, H.; Klene, M.; Li, X.; Knox, J. E.; Hratchian, H. P.; Cross, J. B.; Adamo, C.; Jaramillo, J.; Gomperts, R.; Stratmann, R. E.; Yazyev, O.; Austin, A. J.; Cammi, R.; Pomelli, C.; Ochterski, J. W.; Ayala, P. Y.; Morokuma, K.; Voth, G. A.; Salvador, P.; Dannenberg, J. J.; Zakrzewski, V. G.; Dapprich, S.; Daniels, A. D.; Strain, M. C.; Farkas, O.; Malick, D. K.; Rabuck, A. D.; Raghavachari, K.; Foresman, J. B.; Ortiz, J. V.; Cui, Q.; Baboul, A. G.; Clifford, S.; Cioslowski, J.; Stefanov, B. B.; Liu, G.; Liashenko, A.; Piskorz, P.; Komaromi, I.; Martin, R. L.; Fox, D. J.; Keith, T.; Al-Laham, M. A.; Peng, C. Y.; Nanayakkara, A.; Challacombe, M.; Gill, P. M. W.; Johnson, B.; Chen, W.; Wong, M. W.; Gonzalez, C.; Pople, J. A. *Gaussian 98*, Revision A.3; *Gaussian 03*, Revision B.03; Gaussian, Inc.:Pittsburgh, PA, 2003.

(47) Nguyen, M. T.; Ha, T. K. *J. Am. Chem. Soc.* **1984**, *106*, 599.

(48) Wight, C. A.; Boldyrev, A. I. *J. Phys. Chem.* **1995**, *99*, 12125.

(49) Soto, M. R.; Page, M. *J. Phys. Chem.* **1990**, *94*, 3242.

(50) Alvarez-Idaboy, J. R.; More-Diez, N.; Boyd, R. J.; Vivier-Bunge, A. *J. Am. Chem. Soc.* **2001**, *123*, 2018.

(51) Brucato, J. R.; Palumbo, M. E.; Strazzulla, G. *ICARUS* **1997**, *125*, 135.

(52) Wolfgang, H.; Liedl, K. R.; Hallbrucker, A.; Mayer, E. *Science* **1998**, *279*, 1332.

(53) DelloRusso, N.; Khanna, R. K.; Moore, M. H. *Geophys. Res.* **1993**, *98*, 5505.

(54) Loerting, T.; Tautermann, C.; Kroemer, R. T.; Kohl, I.; Hallbrucker, A.; Mayer, E.; Liedl, K. *Angew. Chem., Int. Ed.* **2000**, *39*, 891.

(55) Zelitch, I. *Annu. Rev. Biochem.* **1975**, *44*, 923.

(56) Silvermann, D. N. *Methods Enzymol.* **1995**, *249*, 479.

(57) Magid, E.; Turbeck, B. O. *Biochim. Biophys. Acta* **1968**, *165*, 515.

(58) Jönsson, B.; Karlström, G.; Wennerström, H. *Chem. Phys. Lett.* **1975**, *30*, 58.

(59) Jönsson, B.; Karlström, G.; Wennerström, H.; Roos, B. *Chem. Phys. Lett.* **1976**, *41*, 317.

(60) Jönsson, B.; Karlström, G.; Wennerström, H.; Forsén, S.; Roos, B.; Almlöf, J. *J. Am. Chem. Soc.* **1977**, *99*, 4628.

(61) Nguyen, M. T.; Ha, T. K. *J. Am. Chem. Soc.* **1984**, *106*, 599.

(62) Nguyen, M. T.; Hegarty, A. F.; Ha, T. K. *J. Mol. Struct.* **1987**, *150*, 319.

(63) Rodwell, W. R.; Bouma, W. J.; Radom, L. *Int. J. Quantum Chem.* **1980**, *18*, 107.

(64) Olkhov, R. V.; Li, Q.; Osborne, M. C.; Smith, I. W. M. *Phys. Chem. Chem. Phys.* **2001**, *3*, 4522.

(65) Good, D. A.; Francisco, J. S. *J. Phys. Chem. A* **2000**, *104*, 1171.
(66) Japar, S. M.; Wallington, T. J.; Richert, J. F. O.; Ball, J. C. *Int. J. Chem. Kinet.* **1990**, *22*, 1257.
(67) Poggi, G.; Francisco, J. S. *J. Chem. Phys.* **2004**, *120*, 5073.
(68) Steinberg, S.; Kawamura, K.; Kaplan, I. *Int. J. Environ. Anal. Chem.* **1985**, *19*, 251.
(69) Sempéré, R.; Kawamura, R. *Atmos. Environ.* **1994**, *28*, 449.
(70) Khwaja, H. A. *Atmos. Environ.* **1995**, *29*, 127.